Available online at www.sciencedirect.com
ScienceDirect
Bioorganic & Medicinal Chemistry 15 (2007) 7688–7695
Bioorganic & Medicinal Chemistry

Elucidation of the RNA target of linezolid by using a linezolid–neomycin B heteroconjugate and genomic SELEX

Hyun Jin Kim, Miyun Kwon and Jaehoon Yu*

Department of Chemistry and Education, Seoul National University, Seoul 151-742, Republic of Korea

Received 1 August 2007; revised 25 August 2007; accepted 28 August 2007
Available online 31 August 2007

Abstract—A covalently modified heteroconjugate between linezolid and neomycin B leads to an enhanced and more specific binding affinity to hairpin RNA targets in comparison to neomycin B itself. This heteroconjugate was used as a lure to select linezolid-specific hairpin RNA from an *Escherichia coli* genome RNA. The selected RNA obtained after eight cycles not only has typical stem–loop structures but also includes known sequences of the linezolid binding site. The results of RNA footprinting show that the binding site of the heteroconjugate encompasses both stem and loop regions, suggesting that the possible binding site for linezolid is in the terminal loop. In addition, findings from application of a surface plasmon resonance assay clearly demonstrate that linezolid binds to selected hairpin RNA in a highly specific manner with a low millimolar affinity. The results suggest that heteroconjugates might represent a generally useful approach in studies aimed at uncovering loop-specific RNA binding ligands that would be otherwise difficult to identify owing to their weak affinities.

1. Introduction

Linezolid, an oxazolidinone antibiotic (Fig. 1), blocks protein synthesis by the inhibition of ribosomal functions.[1] Although several diverse models have been proposed, information about the ribosome binding site for these antibiotics is lacking. One major obstacle to elucidating exact molecular targets of linezolid is their low milli- to sub-millimolar affinities to 70S or 50S ribosomes.[2,3] As a result, the RNA footprinting technique that is commonly used to identify RNA interaction sites has limited utility with these antibiotics.[4] In addition, for the same reason affinity selections have not been seriously explored, except for a photocross-linking method.[5,26]

An indirect method for elucidating drug binding sites involves the analysis of mutant sites in drug-resistant alleles. In the case of linezolid-resistant alleles, mutations are mostly found in the central loop domain V of the peptidyl-transferase center (PTC),[6] which is comprised entirely of 23S rRNA nucleotides both in Gram-positive bacteria[6] and Archaea *Halobacterium halobium*.[7] Recently, drug-resistant mutations were also found in other locations, including a hairpin (stem–loop) structure near the central loop of 23S rRNA.[8] This observation suggests that linezolid has other binding sites in addition to the PTC involved in the inhibition of protein synthesis. Since hairpin structures are the most popular motifs in RNA secondary structures, the recent findings suggest the possibility that linezolid has more than one binding site.

Early efforts to discover biologically relevant RNA motifs have utilized the genomic SELEX (systematic enrichments of ligands by exponentially) procedure[10–12] to identify binding sites of RNA-binding proteins,[9] However, this affinity-based method for the discovery of RNA motifs has been employed only rarely for uncovering small molecule binding sites (e.g., aminoglycosides[13]) probably due to the weak affinities of small molecule ligands to RNA.[14] Recently, we suggested that heteroconjugates might be useful small molecule ligands for hairpin RNAs because they often display sub-high specificities and micromolar binding affinities. In addition, loop-specific interactions have been observed between heteroconjugates and loop sequences in hairpin RNA.[15]

Consequently, we propose that specific novel hairpin RNA motifs can be discovered by using heteroconjugates

Keywords: Linezolid; Neomycin B; Heteroconjugate; Genomic SELEX; Linezolid-specific loop sequences.
* Corresponding author. Tel.: +82 2 880 7761; fax: +82 2 889 0749; e-mail: jhoonyu@snu.ac.kr

0968-0896/$ - see front matter © 2007 Elsevier Ltd. All rights reserved.
doi:10.1016/j.bmc.2007.08.053

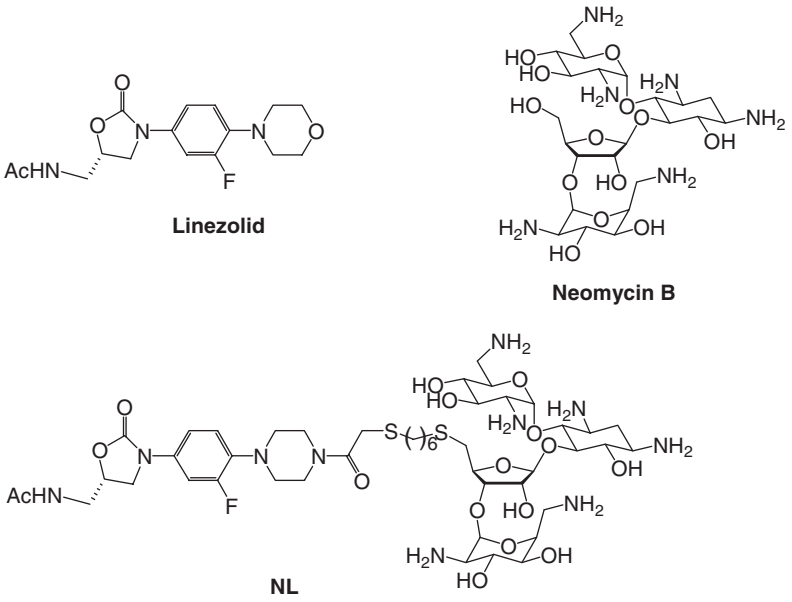

Figure 1. Structures of linezolid, neomycin, and **NL**.

as lures in the affinity-based selection in endogenous RNA. In order to select linezolid-specific sequences in the *Escherichia coli* genome, we have employed a novel neomycin–linezolid heteroconjugate (**NL**, Fig. 1). Three heteroconjugates were designed with spacers of different lengths in the previous study.[15] Binding affinity to the RNA target was dependent on the spacer length and six-carbon spacers had best binding affinity to many RNA targets. Therefore, **NL** with six-carbon spacers was chosen. The results of this study, described below, show that the loop sequence identified by using this heteroconjugate matches a previously reported sequence. The findings suggest that conjugation of small molecules to strong RNA binders will serve as a new strategy for the elucidation of small molecule-specific RNA loop sequences that are otherwise difficult to identify.

2. Results and discussion

2.1. Genomic SELEX

For its use as a lure molecule in the SELEX procedure, the **NL** heteroconjugate was biotinylated.[19] Among several amine functionalities that can be used, aminomethyl groups in the two terminal rings of neomycin B were judged to be the most feasible tethering sites.[20] A genomic RNA library was constructed by employing a modification of the previously described method.[21] Appropriately sized (100–300 bp) purified genomic DNA fragments were chosen,[22] ligated, and PCR amplified by using complement oligonucleotides of 5′ and 3′ constant regions in the vector. In the first round of RNA selection, 10 μg (125 pmol, 7.5×10^{13} molecules) of total RNA was prepared and used.[23] Eight selection cycles against biotinylated **NL** heteroconjugate were performed following the standard SELEX procedure. Selected RNA aptamers were then cloned (Table 1).

2.2. Binding affinities and specificities of drugs against selected aptamers

Among the selected sequences were found multiplicated consensus sequences, such as L2-10 (triplicated), L2-11 (duplicated), and L2-12 (duplicated), accompanied with many single clones (Table 1). L2-17 had the same loop sequence as L2-12 with a little truncated stem, thus, was counted as L2-12. Some of single clones showed weaker binding affinities than the multiplicated clones (data not shown). Further study, therefore, focused on those three sequences. As expected, the predicted secondary structures of all mutiplicated RNA clones have typical stem–loop motifs. Truncated stem–loop hairpin RNA motifs of three mutiplicated aptamers were prepared in order to elucidate the binding region of **NL** heteroconjugate (Fig. 2).

The binding affinities of three truncated hairpin RNAs toward the cognate heteroconjugate were determined by using a fluorescence anisotropy technique.[15] As shown in Table 2, L2-10 and L2-12 of the truncated stem–loop RNA showed relatively stronger binding to the heteroconjugate, while L2-11 displays at least a 3-fold weaker binding affinity. Interestingly, loop sequences of the stronger binders are composed of purines mainly, while that of the weaker binder is populated by pyrimidines (uridines). These findings suggest that the **NL** heteroconjugate preferentially binds to hairpin RNA that has purines in terminal loops. Even though L2-10 showed reasonable affinity owing to neomycin part of **NL** strongly interacts with any RNA aptamer. Based on the fact that the neomycin component of the heteroconjugate targets the stem region, we conclude that linezolid has a binding preference for purine-rich terminal loops.

Among the purine-rich consensus sequences derived from the SELEX, those that have an AAGA sequence

Table 1. Sequences of the selected pools after eight cycles of selection

L2-1	CACGGTTGGCGATGAATGGCGTCACGACAAACTTAGCGATGCTGTGAACCTGACCGGGGAACCAGCTCCAAAACGTCTGCC
L2-5	TGCGAAAATGAGCATTCCGTTCACCCGCCGGCCGAAGAGTTTGCCCCGTCGCTATCGGAAAAAGGCTACTGGCAGGATTTGCCGC
L2-8	GGGCGATGTGAAGCGCGTTGGCTGATCCTTCAACTTCACATCGTAAGTCCCGTACGGTAGACCCC
L2-11	GGTGGTTTTATCCTGGCTGACCAGCTCCTGCTCGCCAATGCGACGATTCTCTTCGTTGTCGCCTTTGACG
L2-14	TTAGCTTTTATGGCGAGTACCTTGCGGGGCACGTCGATAGCTATTTTGCGGTGCTGGTGCGCGTTGGCCTGGCGGCACTCGTTTTTCTGCCGTTTCT
L2-12	GGTCCTGAAGGAACGTTGAAGACGACGTTGAAAGGCCGGGTGTGTAAGCGCAGCGCCTGAGTTTGCGCGTTA
L2-17	TAAGGAACGTTGAAGACGACGTTGAAGGGGTGACCTCTGTGCAGTT
L2-4	TTATCGGTGCGCCGTGGTTCGGGCCAGTGCACTAATG
L2-10	TTATCGGTGCGCCGTGGTTCGGGCCAGTGCACTAATGGGGGCGTTGGGTATTGGGCTGATTATTTTTGTCGATAGCGCCTG
L2-20	TTATCGGTGCGCCGTGGTTCGGGCCAGTGCACTAATGGGGGCGTTGGGTATTGGGCTGATTATTTTTGTCGATAGCGCCT
L2-9	TGTTTTTAATGCTTCAGCGTAATCGGCAGACCAGCCAACGCGCACCAGAAACACGGGCTGACCGCTGGCGCGAAATTTCGCC
L2-16	TGTTTTAATGCTTCAGCGTAATCGGCAGACCAGCCAACGCGCACCAGAAACACGGGCTGACCGCTGGCGCGAAATTTCGCC
L2-6	TCACGTTCAGCGTGCGGGATGGGCGCGGGATTAAAGGACTGATCGGCCATACCCAGCCGCGTCGTCGGCGGCAAGAACAGTGG
L2-13	TCACGTTCAGCGTGCGGGTATGGGCGCGGGATTAAAGGACTGATCGGCCATACCCAGCCGCGTCGTCTGGCGGGCAAGAACAGTGG

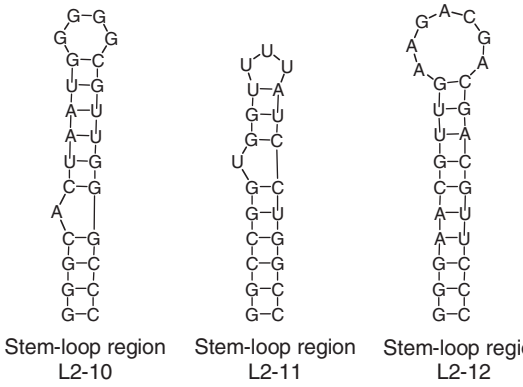

Figure 2. Stem–loop structures of the truncated stem–loop RNA of three consensus aptamers.

Table 2. Dissociation constants (K_d) of neomycin B and **NL** heteroconjugate to RNA aptamers[a]

NL RNA aptamer	Neomycin B	**NL**
L2-10	308 ± 17	90 ± 17
L2-11	313 ± 15	260 ± 7
L2-12	320 ± 60	66 ± 13

[a] Values are in nM. The binding affinities were measured at 20 °C by using a luminescence spectrometer (Perkin-Elmer) and an anisotropy technique.

in terminal loops most strongly bind to the **NL** heteroconjugate. Interestingly, this sequence was already identified as a linezolid binding hairpin motif near PTC (*E. coli* K12 strain, 2054–2070), by observing mutations of the drug-resistant alleles and cross-linking method.[8,26] Thus, this stem–loop RNA was decided to be the subject for further study.

In the fluorescence anisotropy technique, the rhodamine–paromomycin conjugate was used as a probe molecule. Therefore, binding affinities of stem-binders can be calculated based on their ability to replace the fluorescent conjugate. However, the binding affinity of the loop binders, like linezolid, cannot be calculated by using this competition assay.

2.3. Binding affinities and specificities of linezolid against the selected loop

An RNA footprinting method was applied for mapping the binding sites of **NL** and other related drugs on L2-12 hairpin. An autoradiogram from RNA footprinting of L2-12 (Fig. 3) showed that the binding site of neomycin B is in the stem region only, while that of the **NL** heteroconjugate is extended to the terminal loop. The data strongly support the previous conclusion that extension of the binding region for the heteroconjugate is due to the linezolid moiety and that the extended region is likely the linezolid binding site.[15] Importantly, there is little chance that the orientation of **NL** in the stem–loop region is reversed, since neomycin B is a strong stem-binder. However, direct binding of linezolid to either stem or loop regions of RNA could not be observed probably as a result of the weak affinity of the drug.

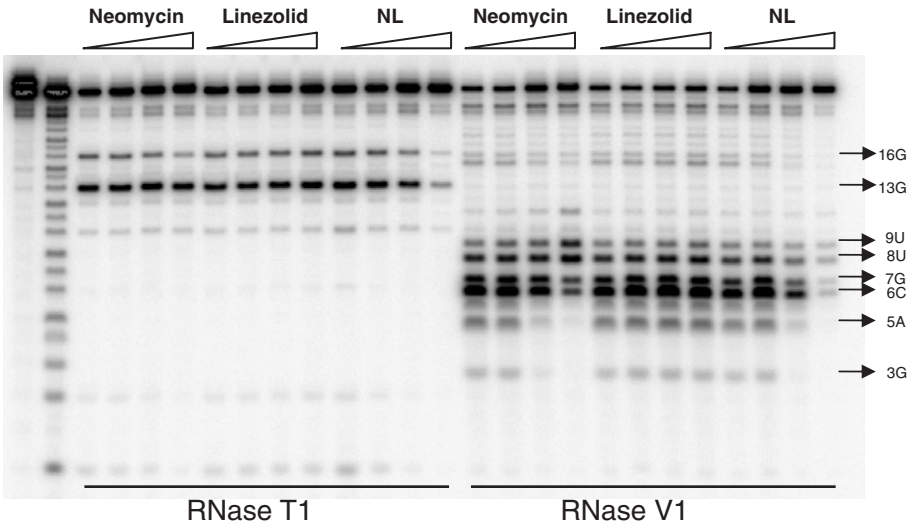

Figure 3. RNA footprinting assay of **NL** aptamer L2-12. Autoradiogram of enzymatic cleavages of **NL** aptamer L2-12 by RNase T1 and RNase V1(Ambion). Lane 1, intact **NL** aptamer L2-12; lane 2, control alkaline hydrolysis; lanes 3–14, containing 0.1 U RNase T1 and about 12 nM of **NL** aptamer L2-12; lanes 3, 7, and 11, RNase T1 control; lane 4, 2.5 μM neomycin B; lane 5, 25 μM neomycin B; lane 6, 250 μM neomycin B; lane 8, 2.5 μM linezolid; lane 9, 25 μM linezolid; lane 10, 250 μM linezolid; lane 12, 2.5 μM **NL**; lane 13, 25 μM **NL**; lane 14, 250 μM **NL**; lanes 15–26, containing 0.1 U RNase V1, about 12 nM of **NL** aptamer L2-12; lane 15, 19, and 23, RNase V1 control; lane 16, 2.5 μM neomycin B; lane 17, 25 μM neomycin B; lane 18, 250 μM neomycin B; lane 20, 2.5 μM linezolid; lane 21, 25 μM linezolid; lane 22, 250 μM linezolid; lane 24, 2.5 μM **NL**; lane 25, 25 μM **NL**; and lane 26, 250 μM **NL**.

In order to directly observe binding of linezolid and related chemicals to the selected RNA, the surface plasmon resonance procedure was employed. By using this technique, even the binding affinities and the specificities of even weak binders can be detected by eluting these substances through immobilized RNA. As shown by the results summarized in Table 3 and Figure 4, linezolid binds to L2-12 with $K_D = 5.4$ mM (but not to L2-11) Even though the binding affinity is low and weak, linezolid must specifically recognize the terminal loop sequence of L2-12.

In order to confirm this proposal, the selective stem-binder neomycin was eluted first through the RNA immobilized chip. This was followed by elution of linezolid. If the binding site of linezolid on L2-12 is occupied by neomycin B, no binding of the former substance would be observed. The observation that linezolid still shows reasonably strong binding ($K_D = 0.45$ mM) to L2-12 when neomycin is present, suggests that the binding sites of the two drugs are different. The comparatively larger binding constant seen in the experiment in which L2-12 is pretreated with neomycin B is probably due to the rigidity of RNA conformation induced by neomycin B. Once again linezolid did not bind to L2-11. This result avoids non-specific interaction between linezolid and L2-12. When combined with footprinting and SPR assay results, observations demonstrate that linezolid is a specific loop binder with a preference for the AAGA sequence.

Table 3. Binding affinities of linezolid and related compounds against RNA aptamers using a BIAcore 3000 instrument[a]

Compound	RNA	k_a (M^{-1} s^{-1})	k_d (s^{-1})	K_D (M)
Neomycin B[b]	L2-11	2.1	1.3×10^{-5}	6.3×10^{-6}
	L2-12	2.3	1.0×10^{-5}	2.3×10^{-6}
NL[b]	L2-11	4.0	3.9×10^{-6}	9.6×10^{-7}
	L2-12	8.7	5.8×10^{-6}	6.7×10^{-7}
Linezolid[c]	L2-11[d]			NB[e]
	L2-12[d]			5.4×10^{-3}
	L2-11[d]			NB[e]
	L2-12[d]			4.5×10^{-4}

[a] RNA was biotinylated and an immobilized streptavidin-coated CM5 sensor chip.
[b] A steady-state 1:1 binding formula or 1:1 binding formula based on simultaneous association/dissociation were used to calculate K_Ds using BIAevaluation 2.1 software (Biacore Inc.).
[c] Binding affinity was calculated from general fitting model using measured steady-state binding level.
[d] Neomycin B was added first, followed by injection of linezolid.
[e] NB, not binding.

The loop region sequence of the highest consensus aptamer is AAGACGA (*E. coli* K-12 strain, 2059–2065). Four bases (AAGA) in this sequence are identical not only with one of the loop sequences (*E. coli* K-12 strain, 2059–2063) in PTC but also with the loop sequence in small hairpin (*E. coli* K-12 strain, 2815–2831) at the vicinity of PTC.[24] Thus, AAGA might represent a general binding sequence for linezolid. However, binding of this drug could be only at a pharmacologically effective AAGA site in the immediate vicinity of PCT, effectively that leads to inhibition of the peptidyl-transferase process.[26] A weak affinity and existence of multiple binding sites might be possible reasons for the relatively high effective concentration of linezolid.

Even though the loop RNA of the selected sequences showed specific and reasonably tight binding for linezolid, a discrepancy exists between the binding affinity we obtained and the reported in vivo and in vitro deter-

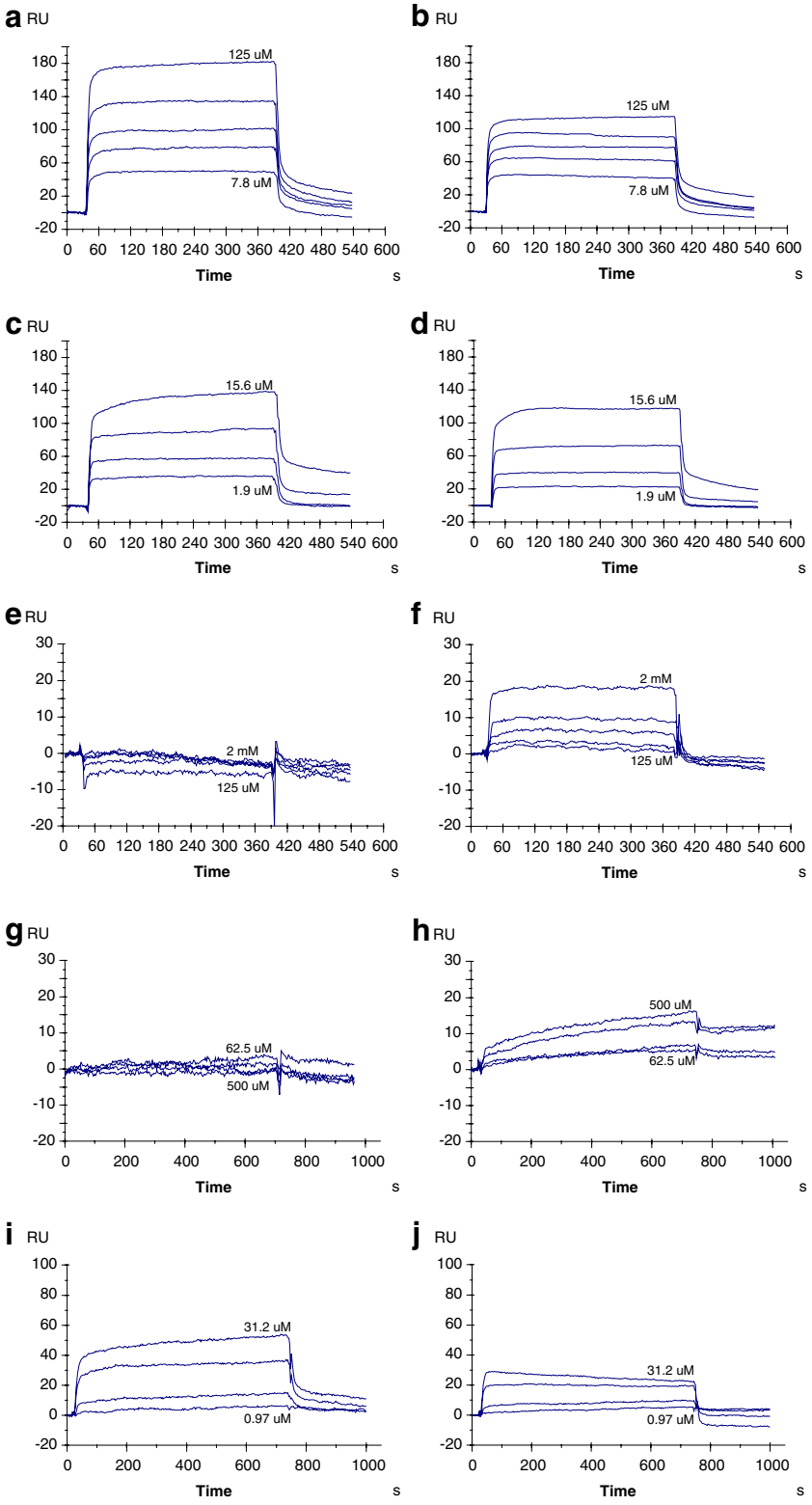

Figure 4. Sensorgrams of linezolid binding to RNA immobilized sensor chip. (a) Neomycin binding against aptamer L2-11; (b) neomycin binding against aptamer L2-12; (c) **NL** binding against aptamer L2-11; (d) **NL** binding against aptamer L2-12; (e) linezolid binding against aptamer L2-11; (f) linezolid binding against aptamer L2-12; (g) linezolid binding against neomycin attached aptamer L2-11; (h) linezolid binding against neomycin attached aptamer L2-12; (i) **NL** binding against neomycin attached aptamer L2-11; (j) **NL** binding against neomycin attached aptamer L2-12.

mined EC_{50} values, which are 1.8 and 20–50 μM, respectively, in *E. coli*.[25] Both of these binding affinities are at least an order of magnitude lower than the EC_{50} observed for the drug against loop RNA. One plausible reason for this discrepancy is that the binding site(s) of the drug is not RNA alone but rather a complex

RNA–protein that is hard to identify by the use of any in vitro methods. Recently, the results of a photo cross-linking experiment indicated that the N-terminus of the L27 protein in ribosomal RNA, located near PCT, is the linezolid binding site.[5,26]

3. Conclusions

A heteroconjugate with linezolid and neomycin was prepared and used as a lure to select stem–loop RNA from an RNA library from *E. coli* genome. Among multiplicated clones obtained by employing the SELEX methodology, L2-12 showed the strongest and most specific binding to the **NL** heteroconjugate. Footprinting and surface plasmon resonance assays showed that linezolid binds weakly but specifically to the L2-12 aptamer, in which an AAGA terminal loop sequence was identified as the possible binding site of the drug. Information gained in this study should help to both unravel the mechanism of linezolid action and advance a new heteroconjugate-based strategy for uncovering new RNA loop specific ligands.

4. Experimental

4.1. Synthesis of NL-biotin

A solution of **NL** (20 mg, 22 μmol) in 50 mM sodium bicarbonate (pH 10) was added to Sulfo-NHS-LC-LC-biotin (15 mg, 1.0 equiv) (PIERCE). The mixture was stirred at 0 °C for 10 h and concentrated, giving a residue which subjected to HPLC using a C18 reverse phase column. Lyophilization of selected fractions gave a powder (17 mg, 35% yield) which was identified as the intended as **NL**-biotin by using MALDI-TOF MS ($M+Na^+$: 1597.7 (calcd), 1597.5 (found)).

4.2. Genomic SELEX

A library from *E. coli* W3110 genomic DNA was constructed for the genomic SELEX method. Although different procedures for construction of genomic libraries have been reported, the method of Stelzl was used.[21] Genomic DNA was isolated by genomic-tip 100/G (Qiagen) and digested by DNase I (Sigma) in the reaction buffer in 50 mM Tris–HCl (pH 8.0), 0.01 mM $MnCl_2$ at 16 °C for 2 h. The plasmid vector pGEM-3Zf(+) was digested with restriction endonuclease SmaI (New England Biolabs) in order to generate blunt ends. Ligation of the digested genomic DNA insert into the vector was performed with T4 DNA ligase (New England Biolabs). In vitro amplification of random genomic DNA fragments by the PCR was performed with primers pGEM-1 (TAATACGACTCACTATAGGGCGAATT CGAGCTCGGTACCC) and pGEM-2 (CCTAGGAG ATCTCAGCTG). RNA library was generated by in vitro transcription with T7 RNA polymerase. After incubation at 37 °C for 4 h, 5 U RQI RNase-free DNase (Promega) were added in order to remove template DNA. RNA was purified on 6% acrylamide–7 M urea gel. RNA fragments ranging in length up to 100-mer were excised and eluted.

A modification of known protocols for the genomic SELEX procedure was used.[13] Ten micrograms of the original RNA library was used for the first selection cycle. For the next selection cycles, 5 μg of RNA was used. RNA was diluted with 100 μL of the binding buffer (140 mM NaCl, 5 mM KCl, 1 mM $MgCl_2$, and 20 mM Hepes at pH 7.5) and denatured for 10 min at 65 °C and allowed to cool to room temperature. The RNA solution was mixed with streptavidin-immobilized agarose beads (Sigma) and incubated for 15 min with gentle vortexing. The solution was carefully transferred to a tube containing appropriate amount of chemicals incubated for 30 min at room temperature. The beads were then washed with binding buffer containing detergent or higher concentration of salt. Binding RNAs were eluted by proper elution buffer (Table 4). RNA was recovered by phenol extraction and ethanol precipitation. The resulting RNA was subjected to RT-PCR for the next selection cycle. RNA was mixed with a pGEM-2 primer and heated at 70 °C for 5 min and cooled to room temperature. M-MuLV reverse transcriptase (Roche) was added with appropriate reaction buffer. The mixture was incubated at 37 °C for 30 min. The resulting cDNA solution was used for the PCR without further purification. PCR was performed by using the same conditions except the reverse-transcribed mixture was employed as a template. After eight cycles of selection, PCR DNA was cloned into pGEM-T-Easy vector (Promega) for sequencing. Selected sequences were analyzed by BLAST web site to find out the genomic regions that contain these sequences. RNA secondary structures were predicted by using the M-FOLD program.[16]

4.3. Measurement of dissociation constants using fluorescence anisotropy

The affinity of the RNA to bind with the cognate molecule was confirmed by using a competition assay with fluorescent anisotropy and CRP (5′-carboxytetramethylrhodamine-labeled paromomycin) as the fluorescence probe.[15] Fluorescence anisotropy measurements were performed on a Perkin-Elmer LS-55 luminescence spectrometer equipped with a thermostat at 20 °C. The tracer solution (100 nM) was excited at 550 nm and monitored at 580 nm. For each single point, eight measurements were made and averaged. The measurements were performed on buffered solutions containing 140 mM NaCl, 5 mM KCl, 1 mM $MgCl_2$, and 20 mM

Table 4. SELEX conditions against **NL** heteroconjugate

Round	Mole ratio (RNA: chemical)	Solid support	Elution buffer condition
1	1:1	Agarose bead	Binding buffer w/2 M NaCl
2	1:1	Agarose bead	Binding buffer w/2 M NaCl
3	1:1	Agarose bead	Binding buffer w/2 M NaCl
4	1:1	Agarose bead	Binding buffer w/2 M NaCl
5	2:1	Agarose bead	Binding buffer w/7 M urea
6	4:1	Polystyrene plate	Binding buffer w/2% SDS
7	4:1	Polystyrene plate	Binding buffer w/2% SDS
8	4:1	Polystyrene plate	Binding buffer w/7 M urea

Hepes (pH 7.5). The equation in the reference was used for the determination of the dissociation constant between RNA and CRP (K_d):

$$A = A_0 + \Delta A\{([\mathrm{RNA}]_0 + [\mathrm{CRP}]_0 + K_d) - ([\mathrm{RNA}]_0 + [\mathrm{CRP}]_0 + K_d)^2 - 4[\mathrm{RNA}]_0[\mathrm{CRP}]_0^{1/2}\}/2$$

where A and A_0 are the fluorescence anisotropies of CRP in the presence and absence of RNA, respectively, ΔA is the difference in concentration of RNA minus the fluorescence anisotropy in the absence of RNA. $[\mathrm{RNA}]_0$ and $[\mathrm{CRP}]_0$ are the initial concentrations of RNA and CRP, respectively. In the competitive binding assay, the following equation was used for the calculation of K_D values:

$$[\mathrm{Chemical}]_0 = \{K_D(A_\Omega - A)/[K_d(A - A_0) + 1]\}\{[\mathrm{RNA}]_0 - K_d(A - A_0)/(A_\Omega - A_0) - [\mathrm{CRP}]_0 \times (A - A_0)/(A_\Omega - A_0)\}$$

Where K_D is the dissociation constant between RNA and the chemical, and $[\mathrm{Chemical}]_0$ is the initial concentration of chemicals. A, A_Ω, and A_0 are fluorescence anisotropic values of the sample, totally bound tracer, and totally free tracer, respectively. Both K_d and K_D were determined by a nonlinear curve fitting using a KaleidaGraph 3.5 software.[15]

4.4. Enzymatic footprinting study

The 5′-end of RNA was dephosphorylated by treatment with calf intestinal alkaline phosphatase (New England Biolabs). ^{32}P was introduced to 5′-position of RNA by T4 polynucleotide kinase (New England Biolabs). The resulting RNA was purified by gel electrophoresis on 15% acrylamide–7 M urea. About 12 nM of trace 5′-^{32}P end-labeled RNA in binding buffer (150 mM NaCl, 5 mM KCl, 1 mM $MgCl_2$, 1 mM $CaCl_2$, and 20 mM Hepes at pH 7.4) were heated to 65 °C for 5 min and slowly cooled to room temperature for 20 min. Appropriate concentrations of chemicals were added to the RNA solution and incubated for 15 min at room temperature. RNase was added to individual tubes. The solutions were incubated for 10 min at 37 °C. The sample was separated on 20% acrylamide–8 M urea gel at 1500 V for 2.5 h and the gel was dried. The gel was exposed and individual bands on the BAS 3000 Phosphorimager (Fujix) and analyzed with Image Reader Ver. 1.3 and Image Gauge Ver. 3.3 software (Fuji photo).

4.5. Surface plasmon resonance analysis

5′-Biotinylated RNA was prepared by introducing phosphorothioate to 5′-position of RNA. RNA was biotinylated with the biotin iodoacetamide derivative.[17] Streptavidin was precoated on flow cells in a CM5 sensor chip (Biacore Inc.) at a flow rate of 5 μL/min using standard NHS/EDC chemistry.[18] After blocking the remaining active sites with ethanolamine, biotinylated RNA was immobilized on a flow cell at a flow rate of 5 μL/min in binding buffer (50 mM Tris–HCl, 150 mM NaCl, 1 mM $MgCl_2$ at pH 7.4). The duration of injection was varied depending on the surface RNA density (about 300 RUs) that was monitored by response unit (RU) value. Neomycin B or linezolid, **NL** in the binding buffer was injected over the RNA surface through multiple rounds at a flow rate of 10 μL/min. Bound compounds were completely removed after each round of injection by flowing 20–60 μL of regeneration buffer (50 mM NaCl) at a flow rate of 10 μL/min over the sensor surface. In order to measure specific binding site of linezolid, neomycin B was injected first and linezolid was injected later. Signals from the reference surface were subtracted from those of the RNA immobilized surfaces.

Acknowledgments

Financial support of this work was provided by Korea Research Foundation (Grant No. 2005-C00264) and Korea Science and Engineering Foundation (Grant No. 2005-01056). H.K. and J.Y. are beneficiaries of the Brain Korea 21 (BK21) program.

References and notes

1. Diekema, D. J.; Jones, R. N. *Lancet* **2001**, *358*, 1575–1582.
2. Zhou, C. C.; Swaney, S. M.; Shinabarger, D. L.; Stockman, B. J. *Antimicrob. Agents Chemother.* **2002**, *46*, 625–629.
3. Barbachyn, M. R.; Ford, C. W. *Angew. Chem.* **2003**, *42*, 2010–2023.
4. Moazed, D.; Noller, H. F. *Nature* **1987**, *327*, 389–394.
5. Colca, J. R.; McDonald, W. G.; Waldon, D. J.; Thomasco, L. M.; Gadwood, R. C.; Lund, E. T.; Cavey, G. S.; Mathews, W. R.; Adams, L. D.; Cecil, E. T.; Pearson, J. D.; Bock, J. H.; Mott, J. E.; Shinabarger, D. L.; Xiong, L.; Mankin, A. S. *J. Biol. Chem.* **2003**, *278*, 21972–21979.
6. Hermann, T. *Curr. Opin. Struct. Biol.* **2005**, *15*, 355–366.
7. Kloss, P.; Xiong, L.; Shinabarge, L. D.; Mankin, A. S. *J. Mol. Biol.* **1999**, *294*, 93–101.
8. Xiong, L.; Kloss, P.; Douthwaite, S.; Andersen, N. M.; Swaney, S.; Shinabarger, D. L.; Mankin, A. S. *J. Bacteriol.* **2000**, *182*, 5325–5331.
9. Gold, L.; Brody, E.; Heilig, J.; Singer, B. *Chem. Biol.* **2002**, *9*, 1259–1264.
10. (a) Singer, B. S.; Shtatland, T.; Brown, D.; Gold, L. *Nucleic Acids Res.* **1997**, *25*, 781–786; (b) Gold, L.; Brown, D.; He, Y.-Y.; Shtatland, T.; Singer, B. S.; Wu, Y. *Proc. Natl. Acad. Sci. U.S.A.* **1997**, *94*, 59–64.
11. Shtatland, T.; Gill, S. C.; Javorvik, B. E.; Johansson, H. E.; Singer, B. S.; Uhlenbeck, O. C.; Zichi, D. A.; Gold, L. *Nucleic Acids Res.* **2000**, *28*, e93.
12. Lee, J. H.; Kim, H.; Ko, J.; Lee, Y. *Nucleic Acids Res.* **2002**, *30*, 5360–5368.
13. (a) Cho, J.; Hamasaki, K.; Rando, R. R. *Biochemistry* **1998**, *14*, 4985–4992; (b) Jiang, L.; Suri, A. K.; Fiala, R.; Patel, D. J. *Chem. Biol.* **1997**, *4*, 35–50; (c) Wallis, M. G.; von Ahsen, U.; Schroeder, R.; Famulok, M. *Chem. Biol.* **1995**, *2*, 543–552; (d) Kwon, M.; Chun, S. M.; Jeong, S.; Yu, J. *Mol. Cell* **2001**, *11*, 303–311.
14. Lin, A. H.; Murray, R. W.; Vidmar, T. J.; Marotti, K. R. *Antimicrob. Agents Chemother.* **1997**, *41*, 2127–2131.
15. Lee, J.; Kwon, M.; Lee, K. H.; Jeong, S.; Hyun, S.; Shin, K. J.; Yu, J. *J. Am. Chem. Soc.* **2004**, *126*, 1956–1957.

16. Mathews, D. H.; Sabina, J.; Zuker, M.; Turner, D. H. *J. Mol. Biol.* **1999**, *288*, 911–940.
17. Wong, C. H.; Liang, F. S. *Methods Enzymol.* **2003**, *362*, 340–353.
18. Johnsson, B.; Lofas, S.; Lindquist, G. *Anal Biochem.* **1991**, *198*, 268–277.
19. The amount of biotin attached was stoichiometrically same as that of **Neo**, judged by the 1H NMR peak integrations of the purified **NL**-biotin.
20. Blanchard, S. C.; Foumy, D.; Eason, R. G.; Puglish, J. D. *Biochemistry* **1998**, *37*, 7716–7724.
21. Stelzl, U.; Nierhaus, K. H. *Methods* **2001**, *25*, 351–357.
22. Zang, W.; Dhen, S. *Biophys. J.* **2006**, *90*, 778–787.
23. A circular DNA of size n can produce n^2 fragments and blunt-end ligation makes two different directions so that the theoretical number of RNA fragments is $2n^2$. We used the fragments ranged from 100 to 300 bp, the diversity of the pool was $2n^2 \times (300 - 100)/n = 400n$. The size of *E. coli* genome is 4.6×106 bp, so the library number is about 2×10^9.
24. Brosius, J.; Dull, T. J.; Sleeter, D. D.; Noller, H. F. *J. Mol. Biol.* **1981**, *148*, 107–127.
25. Shinabarger, D. L.; Marotti, K. R.; Murray, R. W.; Lin, A. H.; Melchior, E. P.; Swaney, S. M.; Dunyak, D. S.; Demyan, W. F.; Buysse, J. M. *Antimicrob. Agents Chemother.* **1997**, *41*, 2132–2136.
26. Leach, K. L.; Swaney, S. M.; Colca, J. R.; McDonald, W. G.; Blinn, J. R.; Thomasco, L. M.; Gadwood, R. C.; Shinabarger, D.; Xiong, L.; Mankin, A. S. *Mol. Cell* **2007**, *26*, 393–402.